Layer dynamics of freely standing smectic-*A* films

Hsuan-Yi Chen and David Jasnow
Department of Physics and Astronomy, University of Pittsburgh, Pittsburgh, Pennsylvania 15260
(Received 27 August 1999)

The dynamics of freely standing thermotropic smectic-*A* films are studied in the isothermal, incompressible limit via a continuous hydrodynamic description. The role of permeation in the films, the structure of the hydrodynamic normal modes, and the form of the autocorrelation functions for the smectic layer and order-parameter fluctuations are discussed. We find two characteristic lengths $l_d=\sqrt{\alpha d/B}$ and $l_c=\sqrt{\eta_3^2 d/8\rho\alpha}$ associated with the dynamic behavior of the system, where α is the surface tension, d is the film thickness, B is the elastic constant for layer compression, η_3 is the layer sliding viscosity, and ρ is the density of the liquid crystal. The crossover from filmlike to bulklike behavior is controlled by l_d alone; the crossover from overdamped to underdamped dynamics when the in-plane length scale is large compared to l_d is controlled by l_c alone.

PACS number(s): 61.30.Cz, 68.15.+e, 83.70.Jr

I. INTRODUCTION

A three-dimensional smectic-*A* phase has a layered structure with one-dimensional order along the layering direction and fluidlike behavior within the layers. Choosing the z axis to be the symmetry-breaking direction, to linear order the bulk elastic free-energy density is given by [1,2]

$$f_b=\frac{1}{2}\left\{B\left(\frac{\partial u}{\partial z}\right)^2+K_1\left(\frac{\partial^2 u}{\partial x^2}+\frac{\partial^2 u}{\partial y^2}\right)^2\right\}, \tag{1}$$

where $u(\mathbf{r},t)$ is the layer displacement, $\mathbf{r}=(x,y,z)$, and B and K_1 are, respectively, the layer compression and undulation elastic moduli. Since a uniform rotation around any axis in the xy plane costs no energy, there is no $(\partial u/\partial x)^2+(\partial u/\partial y)^2$ term in the elastic energy. As a result, the layer displacement fluctuations diverge logarithmically with the size of the system, and the smectic-*A* phase is at its lower critical dimension. However, the divergence is sufficiently weak that finite-size effects stabilize laboratory samples [1].

With their high degree of uniformity and easily controlled thickness, freely standing smectic films are often used to study the finite-size and boundary effects for systems at their lower critical dimensions. Experimental and theoretical studies on the static [3–5], dynamic [6–8], and off-equilibrium [9] properties of freely standing smectic-*A* films show very interesting behavior; some features are drastically different from bulk smectic systems, while some represent crossover from two-dimensional to three-dimensional behavior.

In this paper we introduce a continuum theory for the hydrodynamics of a *thermotropic* smectic-*A* film in the isothermal, incompressible limit based on the linear hydrodynamic theory constructed by Martin *et al.* [10]. Our study provides a finite-thickness counterpart to the hydrodynamic theory for bulk smectic-*A* systems. We clarify the appropriate boundary conditions for the equations of motion, discuss the role of permeation close to the free surfaces, compare the structure of hydrodynamic normal modes with that of bulk systems, and provide a theoretical picture for the dynamic crossover behavior of a freely standing smectic-*A* film from a thin film, with properties similar to an ordinary fluid film, to a three-dimensional system with layer structure.

In Sec. II we briefly review the linear-response functions of the surfaces of a smectic-*A* film [11]. We show that the dynamic properties of the smectic layers in a freely standing film can be extracted from the surface response functions. Since the layer displacement for a smectic-*A* film has to satisfy certain boundary conditions on the free surfaces, the normal modes for the dynamics of the layers depend on both surface and bulk properties.

The crossover of the smectic-layer dynamics from filmlike behavior to bulklike behavior is discussed in Sec. III. Two lengths, $l_d=\sqrt{\alpha d/B}$ and $l_c=\sqrt{\eta_3^2 d/8\rho\alpha}$ with $l_c \gg l_d$, are shown to characterize the dynamics of the system, where α is the surface tension, d is the thickness of the film, ρ is the density, and η_3 is the in-plane shear viscosity [10]. We emphasize that when the in-plane wavelength ($\sim q_\perp^{-1}$) is large compared to l_d, the behavior of the system is similar to an ordinary liquid film, and when $q_\perp l_c \ll 1$, the layer dynamics of the system is underdamped. The characteristic time scale for a long in-plane wavelength ($q_\perp l_d \ll 1$) is shown to be $\tau_0=\eta_3 d/2\alpha$. The effects of the smectic-layer structure can be found in short-time ($t \ll \tau_0$), short-wavelength ($q_\perp l_d \gg 1$) behavior. This is supported by a recent study of the smectic order-parameter autocorrelation function for free-standing smectic-*A* films [7], where a scaling form for the correlation function is proposed and studied numerically with a discrete model. As discussed in Sec. IV, our continuum theory provides the conceptual background for such behavior with a clear picture based on the behavior of the hydrodynamic normal modes.

In Sec. V we summarize results and add concluding remarks. Some additional details on permeation near the surfaces and the calculation of the dynamic correlation functions are provided in Appendixes A, B, and C, respectively.

The material parameters, characteristic lengths, time scales, as well as dimensionless numbers are listed in Table I with their definitions and typical values.

II. HYDRODYNAMIC NORMAL MODES OF A FREELY STANDING SMECTIC-*A* FILM

We consider a freely standing smectic-*A* film which extends from $z=d/2$ to $z=-d/2$ in the vertical direction and is

TABLE I. Parameters and magnitudes.

	Parameter definition	Physical meaning	Magnitude
B		layer compressibility	2.5×10^7 dyn/cm^2
K_1		layer undulation modulus	10^{-6} dyn
ρ		smectic-A density	1 g/cm^3
η_3		in-plane shear viscosity	1 P
α		surface tension	30 dyn/cm
g	$\alpha/\sqrt{K_1 B}$		$O(1)$
λ	$\sqrt{K_1/B}$	penetration length	10^{-7} cm
d		smectic-A film thickness	
l_d	$\sqrt{\alpha d/B}$ $=\sqrt{g\lambda d}$	length which separates filmlike and bulklike behavior	$l_d\sim\sqrt{\lambda d}$
l_c	$\sqrt{\eta_3^2 d/8\rho\alpha}$	length which separates underdamped and overdamped dynamics in $q_\perp l_d\ll1$ regime	$l_c\gg l_d$ $(l_c/l_d\sim50)$
τ_0	$\eta_3 d/2\alpha$	lifetime for overdamped $n=0$, $q_\perp l_d\ll1$ modes	

of infinite extent in the x and y directions. The geometry of the system is shown in Fig. 1, which shows $\zeta^{+\,(-)}$ as the displacement of the upper (lower) surface from its equilibrium position. In the absence of external fields, the smectic layers are always aligned and parallel to both free surfaces. In this section we first briefly review previous results [11] on the derivation of the linear-response function for the equilibrium surface fluctuations of a freely standing smectic-A film in the low-frequency, long-wavelength regime [13,14], and then extend these results to the structure of hydrodynamic normal modes of the system.

Suppose the system were perturbed by external forces with fixed in-plane wave vector $\mathbf{q}_\perp$ and frequency ω on both upper and lower surfaces, i.e.,

$$P^+_{\rm ext}(\mathbf{r}_\perp,t)=P^+_{ext}(\mathbf{q}_\perp,\omega)e^{i\mathbf{q}_\perp\cdot\mathbf{r}_\perp-i\omega t},$$
$$P^-_{\rm ext}(\mathbf{r}_\perp,t)=P^-_{\rm ext}(\mathbf{q}_\perp,\omega)e^{i\mathbf{q}_\perp\cdot\mathbf{r}_\perp-i\omega t}. \tag{2}$$

We look for the linear-response functions of the surfaces in the regime of weak external forces.

In the absence of topological defects, under constant temperature and assuming incompressibility, to linear order the system satisfies the equations of motion [1,2]

$$\rho\frac{\partial v_i}{\partial t}=-\partial_i p+\partial_j\sigma'_{ij}+h\,\delta_{iz}, \tag{3}$$

$$\frac{\partial u}{\partial t}=v_z+\zeta_p h, \tag{4}$$

where v_i is the ith component of the velocity field, and the pressure, p, is actually a Lagrange multiplier for the incompressibility condition. The viscous stress tensor is denoted by σ' [10], ζ_p is the permeation constant, and the molecular field h in linear theory is defined by

$$h\equiv B\partial_z^2 u-K_1\partial_\perp^2\partial_\perp^2 u=B(\partial_z^2-\lambda^2\partial_\perp^2\partial_\perp^2)u, \tag{5}$$

where $\lambda=\sqrt{K_1/B}$ is the penetration length [1] and $\partial_\perp^2=\partial_x^2+\partial_y^2$. In Eq. (3) we sum on repeated indices, and $\partial_j=\partial/\partial x_j$.

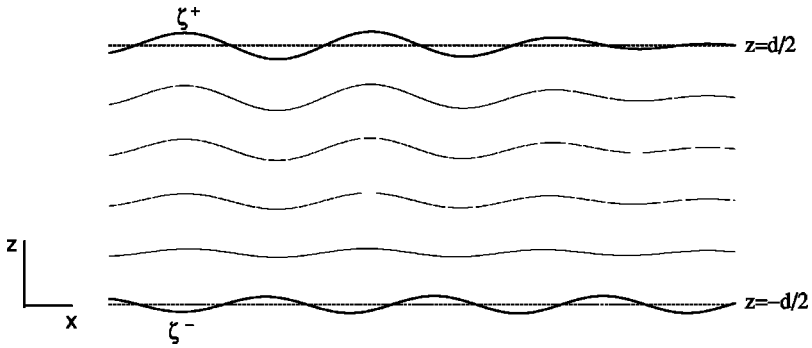

FIG. 1. Schematic of a freely standing smectic-A film of thickness d. The y axis points into the paper. The dotted lines are the equilibrium positions of the free surfaces.

On the free surfaces the system has to satisfy the following boundary conditions.

BC1. The velocity of the free surfaces is the same as the normal component of the liquid crystal velocity on the surfaces.

BC2. For free surfaces the normal component of the permeation force should vanish [11].

BC3. The force acting on the system is continuous across the free surfaces.

The boundary conditions lead to the following equations for the system:

$$\frac{\partial \zeta^{\pm}}{\partial t} = [v_z]_{z=\pm d/2}, \tag{6}$$

$$\left[\frac{\partial u}{\partial z}\right]_{z=\pm d/2} = 0, \tag{7}$$

$$[\partial_i v_z + \partial_z v_i]_{z=\pm d/2} = 0, \quad i = x,y, \tag{8}$$

$$\left[\pm\left(-p + 2\eta_3 \frac{\partial v_z}{\partial z} + B\frac{\partial u}{\partial z}\right) - \alpha \nabla_{\perp}^2 \zeta^{\pm} - P_{\text{ext}}^{\pm}\right]_{z=\pm d/2} = 0. \tag{9}$$

Solving Eqs. (3) and (4) with these boundary conditions, one finds that, in the presence of the driving forces with given $q_\perp$ and ω, there are four different q_z's. One of them is associated with the diffusive motion of v_x and v_y, and is decoupled from the motion of u and v_z; hence, it is irrelevant for the calculation of surface response functions (see BC1). Another two values of q_z are associated with permeation, and these contributions to the layer displacement are small (see Appendix A). The last of these q_z values dominates the contribution to the smectic-layer displacement; hence u can be approximated by

$$u(\mathbf{r},t) = u_S(\mathbf{q}_\perp,\omega)\cos[q_z(q_\perp,\omega)z] \times e^{i\mathbf{q}_\perp\cdot\mathbf{r}_\perp - i\omega t} + u_A(\mathbf{q}_\perp,\omega)\sin[q_z(q_\perp,\omega)z] \times e^{i\mathbf{q}_\perp\cdot\mathbf{r}_\perp - i\omega t}, \tag{10}$$

where $|q_z| \ll q_\perp$ and, in general, $q_z(q_\perp,\omega)$ is complex under the conditions considered [13]. It is determined by the solution of the following with Re $q_z > 0$:

$$i\omega = i\omega_{\pm}(q_\perp, q_z), \tag{11}$$

where

$$i\omega_{\pm}(q_\perp,q_z) = \frac{\eta_3 q_\perp^2}{2\rho}\left(1 \pm \sqrt{1 - \frac{4\rho}{\eta_3^2 q_\perp^4}(Bq_z^2 + K_1 q_\perp^4)}\right), \tag{12}$$

and η_3 is one of the five viscosity coefficients characterizing a smectic A [10].

When $P_{\text{ext}}^{+} = P_{\text{ext}}^{-}$ ($P_{\text{ext}}^{+} = -P_{\text{ext}}^{-}$), the dynamics of the system are symmetric (antisymmetric) under $z \to -z$, and the layer displacement is described by u_S (u_A) alone. The response functions for both symmetric and antisymmetric surface motions are defined by

$$\zeta^S(q_\perp,\omega) = X^S(q_\perp,\omega)[P_{\text{ext}}^{+}(q_\perp,\omega) + P_{\text{ext}}^{-}(q_\perp,\omega,)],$$
$$\zeta^A(q_\perp,\omega) = X^A(q_\perp,\omega)[P_{\text{ext}}^{+}(q_\perp,\omega) - P_{\text{ext}}^{-}(q_\perp,\omega,)], \tag{13}$$

where

$$\zeta^{S(A)} = \frac{1}{2}(\zeta^{+} \pm \zeta^{-}). \tag{14}$$

A calculation from the continuum hydrodynamics leads to the following expressions for the response functions [11]:

$$X^S = \frac{1}{2}\,\frac{1}{\alpha q_\perp^2 - Bq_z(q_\perp,\omega)\tan[dq_z(q_\perp,\omega)/2]}, \tag{15}$$

$$X^A = \frac{1}{2}\,\frac{1}{\alpha q_\perp^2 + Bq_z(q_\perp,\omega)\cot[dq_z(q_\perp,\omega)/2]}. \tag{16}$$

It appears that permeation processes have no contribution to the dynamics of the surfaces in the regime [13] where our analysis is done. However, the solution for $u(\mathbf{r},t)$ in Eq. (10) does not strictly satisfy BC2. This means that the contribution from permeation enables the system to satisfy the boundary conditions [12] but otherwise has little significance. The role of permeation in the dynamics of the system is discussed in further detail in Appendix A.

The response functions $X^{S(A)}$ have been derived as functions of the in-plane wave vector $q_\perp$ and frequency ω of the applied external forces. One can also define ω in the complex plane; then the poles of the response functions provide the natural frequencies of the surface fluctuations in the absence of driving forces [2]. In linear theory these poles also reveal the frequencies of layer displacement. Each pole in the complex ω plane corresponds to a hydrodynamic normal mode associated with the layer displacement. Since we are not interested in the dynamics of v_x and v_y, which decouple from the dynamics of u and v_z, these poles provide the information of interest.

Defining dimensionless parameter $g = \alpha/\sqrt{K_1 B}$ [15] and characteristic length $l_d = \sqrt{\alpha d/B} = \sqrt{g\lambda d} \sim \sqrt{\lambda d}$, one finds for given $q_\perp$, that the normal modes satisfy the following equation:

$$q_z d = \pm (q_\perp l_d)^2 \left[\cot\left(\frac{q_z d}{2}\right)\right]^{\pm 1}. \tag{17}$$

Thus the z dependence of the normal modes is determined, and the frequencies of the normal modes are determined in turn by Eq. (11). One also finds that the normal modes have definite symmetry under $z \to -z$; the normal modes associated with the ''$+(-)$'' sign in Eq. (17) are symmetric (antisymmetric) under $z \to -z$. The form of the layer displacement in Eq. (10) suggests that, for given $\mathbf{q}_\perp$, the layer displacement for a normal mode is an eigenfunction of the differential equation

$$\frac{\partial^2 \psi(\mathbf{q}_\perp,z)}{\partial z^2} = -q_z^2 \psi(\mathbf{q}_\perp,z) \tag{18}$$

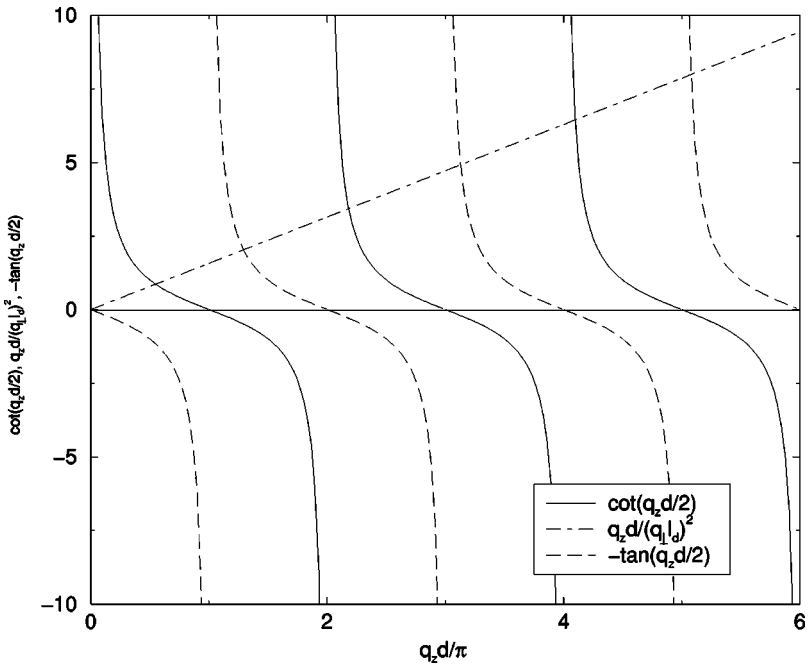

FIG. 2. Graphical solution for the q_z's for dimensionless parameter $q_\perp l_d=\sqrt{2}$. The abscissa in all cases is $q_z d/\pi$. The three functions plotted are $q_z d/(q_\perp l_d)^2$ (dot-dashed line), $\cot(q_z d/2)$ (solid lines), and $-\tan(q_z d/2)$ (dashed lines). The crossings of the dot-dashed line and the solid lines give the values of $q_z^{(n)} d/\pi$ for normal modes with n even; the crossings of the dot-dashed line and the dashed lines (except the origin) give the values of $q_z^{(n)} d/\pi$ for normal modes with n odd.

with boundary condition BC2′:

$$\left[B\frac{\partial\psi(\mathbf{q}_\perp,z)}{\partial z}\pm\alpha\ \ q_\perp^2\psi(\mathbf{q}_\perp,z)\right]_{z=\pm d/2}=0. \tag{19}$$

It is straightforward to show that these eigenfunctions form a complete basis for the interval $-d/2<z<d/2$. The apparent contradiction between BC2′ and BC2 is discussed in Appendix A.

In general, q_z in Eq. (17) cannot be determined analytically. However, the q_z's are all real, and we can choose them to be positive. The graphical solutions for the q_z's are shown in Fig. 2. We label the q_z's for the normal modes as $q_z^{(n)}(q_\perp)$, $n=0,1,2,\ldots$ with $q_z^{(0)}(q_\perp)<q_z^{(1)}(q_\perp)<q_z^{(2)}(q_\perp)<\ldots$, and note that there are two normal modes associated with each $q_z^{(n)}$. The layer displacement for normal modes is even (odd) under $z\rightarrow -z$ if n is even (odd). The layer displacement for the normal modes with $n=0$ is even under $z\rightarrow -z$.

To compare with the behavior of a bulk smectic A, recall that translational invariance of the bulk system allows one to label modes by a d-dimensional wave vector. For a freely standing smectic-A film, the boundary conditions and the equations of motion select a set of normal modes for the dynamics of the system. We can express the normalized time-independent part of the normal modes in the following way:

$$\psi(\mathbf{q}_\perp,n;z)=N(q_\perp,n)\cos[q_z^{(n)}(q_\perp)z]\ \text{for}\ n=0,2,4,\ldots \tag{20}$$

and

$$\psi(\mathbf{q}_\perp,n;z)=N(q_\perp,n)\sin[q_z^{(n)}(q_\perp)z]\ \text{for}\ n=1,3,5,\ldots, \tag{21}$$

where

$$N(q_\perp,n)=\sqrt{\frac{2}{d}}\left(1+(-1)^n\frac{\sin(q_z^{(n)}d)}{q_z^{(n)}d}\right)^{-1/2}. \tag{22}$$

These normal modes satisfy the orthonormality condition

$$\int_{-d/2}^{d/2}dz\ \psi(\mathbf{q}_\perp,n;z)\psi(\mathbf{q}_\perp,m;z)=\delta_{mn}. \tag{23}$$

Hence, these modes can be used as a basis to expand any $u(\mathbf{q}_\perp,z,t)$ as

$$u(\mathbf{q}_\perp,z,t)=\sum_n\ u(\mathbf{q}_\perp,n,t)\times\psi(\mathbf{q}_\perp,n;z). \tag{24}$$

As discussed in Appendix B, the general form for the dynamic correlation function of u is

$$c(q_\perp,n,t)\equiv\langle u(q_\perp,n,t)u(-q_\perp,n,0)\rangle = \frac{i\omega_+e^{-i\omega_-t}-i\omega_-e^{-i\omega_+t}}{i\omega_+-i\omega_-}\frac{k_BT}{Bq_z^{(n)2}+K_1q_\perp^4}, \tag{25}$$

where $\omega_\pm=\omega_\pm(q_\perp,q_z^{(n)})$ is related to $q_\perp$ and $q_z^{(n)}$ through Eq. (12).

In summary, we find that in common with analysis of a liquid film, the normal modes are symmetric or antisymmetric under $z\rightarrow -z$. They also are labeled by $(\mathbf{q}_\perp,n)$, and the layer displacement can be treated as eigenfunctions of a differential equation. The frequencies for those normal modes can be obtained from the poles of the *surface response functions* in the complex ω plane. As will become clear in the next section, the difference between those $q_z^{(n)}$'s which correspond to the normal modes for a finite thickness smectic-A film and the set of numbers $(n+1)\pi/d$, $n=0,1,2,\ldots$ provides a measure of the degree to which finite thickness and surface tension change the dynamic properties of the layer

displacement. Experimentally, these effects are typically observed by measuring the frequencies and the magnitude of the autocorrelation function of the layer displacement. Layer dynamics will be discussed further in the following section.

III. CROSSOVER OF LAYER DYNAMICS FOR SMECTIC-A FILMS

Equation (17) shows that the q_z's of the hydrodynamic normal modes depend only on the dimensionless parameter $q_\perp l_d$ and the thickness d, and they can be expressed as

$$q_z^{(n)} = \frac{1}{d} f_n(q_\perp l_d). \tag{26}$$

When $q_\perp l_d \ll 1$,

$$f_0(q_\perp l_d) \approx \sqrt{2} l_d \ q_\perp ,$$

$$f_n(q_\perp l_d) \approx n\pi \left[1 + 2\left(\frac{l_d}{n\pi} \right)^2 q_\perp^2 \right], \quad n = 1,2,3, \ldots , \tag{27}$$

while when $q_\perp l_d \gg 1$,

$$f_n(q_\perp l_d) \approx (n+1)\pi \left[1 - \frac{2}{(l_d q_\perp)^2} \right], \quad n = 0,1,2,3, \ldots . \tag{28}$$

For intermediate $q_\perp l_d$, the behavior of $f_n(q_\perp l_d)$ is complicated and must be analyzed numerically.

A. $q_\perp l_d \ll 1$ regime

The dynamics of the smectic layers when $q_\perp l_d \ll 1$ are dominated by the $n=0$ modes. This can be understood by comparing the magnitude and characteristic time scales of the correlation functions. The condition $q_\perp l_d \ll 1$ is satisfied for typical materials when $q_\perp^2 d \ll B/\alpha \sim 10^6$ cm^{-1}. On the other hand, the molecular field h [Eq. (5)] for the $n=0$ modes is dominated by the $B\partial_z^2 = -B(q_z^{(0)})^2$ term when $q_\perp^2 d \ll \alpha/K_1 \sim 3\times 10^7$ cm^{-1}. Since from Eq. (27) the magnitude of q_z satisfies $q_z^{(0)} \ll q_z^{(n)}$ for all $n>0$ when $q_\perp l_d \ll 1$, one finds that $c(q_\perp,0,0) \gg c(q_\perp,n,0)$ for all $n>0$ from Eq. (25), and the molecular field in this regime is dominated by the contribution from the $B\partial_z^2$ term. Furthermore, from Eq. (12), one finds that the $n=0$ modes have much longer characteristic time scales than the $n>0$ modes. Hence, for $l_d q_\perp \ll 1$, the $n=0$ modes dominate the dynamics of the smectic layers. Substituting $q_z^{(0)}$ into Eq. (12), one finds

$$i\omega_\pm(q_\perp, q_z^{(0)}) = \frac{\eta_3 q_\perp^2}{2\rho} \left[1 \pm \sqrt{1 - \left(\frac{1}{q_\perp l_c} \right)^2} \right], \tag{29}$$

where $l_c = \sqrt{\eta_3^2 d/8\rho\alpha}$ is instrumental in determining whether the layer oscillations are overdamped or underdamped. Notice that $\omega_\pm(q_\perp, q_z^{(0)})$ is independent of the bulk elastic constants; hence the dynamic behavior of the system in the $q_\perp l_d \ll 1$ regime resembles that of an ordinary fluid film. When $l_c q_\perp \gg 1$, the $n=0$ normal modes are strongly *overdamped* with decay rates

$$i\omega_+^{(0)}(q_\perp) = \frac{\eta_3 q_\perp^2}{\rho}, \qquad i\omega_-^{(0)}(q_\perp) = \frac{2\alpha}{\eta_3 d} \equiv \tau_0^{-1} \ll i\omega_+^{(0)}(q_\perp). \tag{30}$$

Since we are interested in slow modes of the system, $i\omega_-^{(0)}(q_\perp) \equiv \tau_0^{-1}$ provides the characteristic time for the system, and the autocorrelation function for layer fluctuations has the form

$$c(q_\perp,0,t) \approx \frac{k_B T d}{2\alpha q_\perp^2} e^{-t/\tau_0} \text{ for } l_c q_\perp \gg 1 \gg l_d q_\perp . \tag{31}$$

Notice that τ_0 is independent of $q_\perp$. This particular time scale controls the dynamics in the $l_d \ll q_\perp^{-1} \ll l_c$ regime, and it arose in previous experimental, numerical, as well as theoretical studies [6,7]. When $l_c q_\perp \ll 1$, the $n=0$ normal modes are *underdamped* with decay rate $2(q_\perp l_c)^2 \tau_0^{-1}$ and frequency $\sqrt{2\alpha/\rho d}\, q_\perp = 2 q_\perp l_c \tau_0^{-1}$. As $q_\perp \to 0$, the damping is small; this is the regime in which the long-wavelength theory and corresponding experiments [16] have been performed. The autocorrelation function for layer fluctuations in this regime is given by

$$c(q_\perp,0,t) \approx \frac{k_B T d}{2\alpha q_\perp^2} \cos(2 q_\perp l_c t/\tau_0) e^{-2(q_\perp l_c)^2 t/\tau_0} \qquad (l_d q_\perp \ll l_c q_\perp \ll 1). \tag{32}$$

The behavior of the $n=0$ eigenfunction $\psi(q_\perp,0;z)$ is simple when $l_d q_\perp \ll 1$, namely,

$$\psi(q_\perp,0;z) = \sqrt{\frac{1}{d}} + O\left(\left(q_\perp l_d \frac{z}{d} \right)^2 \right), \tag{33}$$

which has a very weak z dependence. It has been pointed out that the static properties of the smectic-A layer fluctuations in a film with $q_\perp l_d \ll 1$ are z independent [3]; here we have shown that a similar property holds for the dynamics as well.

We have shown that the physical properties of the system in the $q_\perp l_d \ll 1$ regime are similar to a *simple fluid film*. The dynamics of the system show a competition between the elasticity due to *surface tension* and viscous loss characterized by the coefficient η_3. The underdamped motion of a smectic-A *film* should not be confused with ''second sound'' for smectic layers, because for long in-plane wavelength the layer compression is negligible. In this regime, the underdamped motion is simply the vibration of a simple fluid film with surface tension α. Also notice that although the magnitude of $q_z^{(0)}$ depends on the elastic constant B, this dependence does not show up in the dynamical correlation function for the hydrodynamic normal modes, as can be checked by substituting $q_z^{(0)}$ into Eq. (25).

To probe the crossover behavior of the film, experiments have to be performed outside the $q_\perp l_d \ll 1$ regime so that the effect of the bulk elasticity can be revealed. This can be done by increasing the film thickness or adjusting the relevant in-plane wave vector. When $q_\perp l_d$ increases to order unity,

the layer structure of the system starts to play a non-negligible role in the system. The layer fluctuations of the normal modes with $n>0$ become comparable to the layer fluctuations for the $n=0$ modes. Hence, the dynamics of the layers for fixed $q_\perp$ are no longer simply controlled by $\omega_\pm(q_\perp, q_z^{(0)})$. The first sign of this crossover behavior can be detected by exciting the $n=1$ modes. As pointed out in the study of the surface dynamics of freely standing smectic-*A* films [11,17], this pair of modes is similar to the so-called *peristaltic* mode for a soap film. However, the characteristic time scales of these modes strongly depend on the elasticity of the smectic layers; hence, the dynamic properties of these modes actually reveal the difference between a smectic film and a soap film. The possibility of surface light-scattering experiments for probing these normal modes is also discussed in Ref. [11].

B. $q_\perp l_d \gg 1$ regime

In the opposite limit, $q_\perp l_d \gg 1$, the q_z's for all normal modes can be approximated by a single expression, Eq. (28). One finds that, in this limit, the eigenfunctions for the normal modes, given in Eqs. (20) and (21), vanish on both free surfaces as $(q_\perp l_d)^{-1} \to 0$. This means that, in this limit, the layer displacement is not affected by the surface tension. The dynamics of the layers when $q_\perp l_d \gg 1$ is similar to that of a bulk smectic *A* with thickness *d*, except very close to the free surfaces. This can be seen from the fact that the $q_z^{(n)}$'s take values approximately equal to $(n+1)\pi/d$, with a finite-size correction. When $4\rho(Bq_z^{(n)2}+K_1 q_\perp^4)/\eta_3^2 q_\perp^4 \ll 1$, the motion of the layers is strongly *overdamped*. For given $q_z^{(n)}$ and $q_\perp$, there are two modes. The slow one, which corresponds to layer undulation, has

$$
\begin{aligned}
i\omega_-(q_\perp, q_z^{(n)}) &= \frac{Bq_z^{(n)2}+K_1 q_\perp^4}{\eta_3 q_\perp^2} \\
&\approx \frac{[(n+1)\pi]^2+\lambda^2 d^2 q_\perp^4}{\lambda d q_\perp^2}(g\tau_0)^{-1} \\
&> \lambda d q_\perp^2 (g\tau_0)^{-1} \gg \tau_0^{-1}, \qquad (34)
\end{aligned}
$$

where we have used the fact that $\lambda d \sim l_d^2$ and $g \sim O(1)$ for typical materials. The fast decay mode now corresponds to the diffusive mode for v_z. Notice that, similar to bulk systems [1], the dominant fluctuations in this regime come from the modes with $B(q^{(n)})^2 \sim K_1 q_\perp^4$, i.e., $n \sim \lambda d q_\perp^2/\pi \gg 1$; the boundary conditions have little effect on the *z* dependence of these modes, and their dynamics are *overdamped*.

To study the dynamics of the smectic-*A* film in the $q_\perp l_d \gg 1$ regime for typical laboratory materials, we need $q_\perp^2 d \gg B/\alpha \sim 10^6$ cm^{-1}. For $d \sim 10^{-3}$ cm, which can be achieved easily, the momentum transfer in the *xy* plane should be at least of order 10^5 cm^{-1}, which can also be achieved.

The crossover of the dynamics for the system is illustrated in Fig. 3, where the normalized dynamic correlation functions $C(q_\perp, n, t) = c(q_\perp, n, t)/c(q_\perp, 0, 0)$ for normal modes with $n = 0,1,2,3$, are shown for a smectic-*A* film with thickness $d = 10$ μm, and typical elastic coefficients and viscosities. The in-plane wave vector $q_\perp$ is chosen such that the dimensionless parameter $(l_d q_\perp)^{-2} = B/\alpha q_\perp^2 d$ is 20 000, 2000, 1, and 0.1, respectively. When $(l_d q_\perp)^{-2} = 20\,000$, the normal modes with $n>0$ are negligible, and $n=0$ normal modes are underdamped, as one can check that $q_\perp l_c = 5/12 < 1$. For $(l_d q_\perp)^{-2} = 2000$, the $n>0$ normal modes are still negligible, but the $n=0$ normal modes are overdamped with a decay which is not a single exponential. This occurs when the two time scales are close to each other, as illustrated in Fig. 4 near the point of critical damping. For $(l_d q_\perp)^{-2} = 1$, the normal modes with $n>0$ can be observed; this is the crossover regime. For $(l_d q_\perp)^{-2} = 0.1$, the contribution from bulk elasticity is sufficiently large that the dynamic correlation functions for normal modes with $n>0$ are easily seen in the figure. Similarly to the undulation mode in bulk systems, all normal modes decay exponentially. This is the overdamped limit of the $q_\perp l_d \gg 1$ regime. The actual $q_\perp$ values in

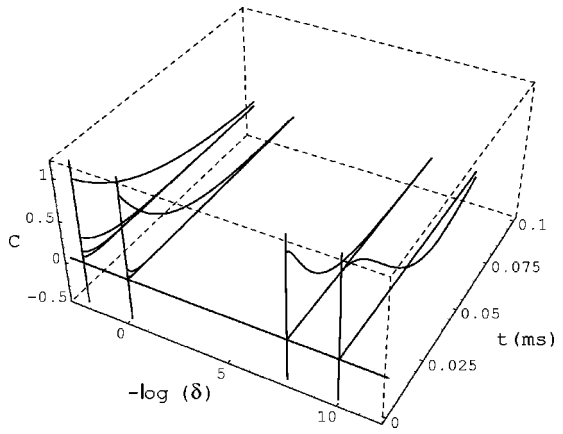

FIG. 3. Dimensionless dynamic correlation function $C(q_\perp, n, t) \equiv c(q_\perp, n, t)/c(q_\perp, 0, 0)$ for $n = 0,1,2,3$. The material parameters are chosen to be $d = 10$ μm, $B = 2.5 \times 10^7$ dyn/cm^2, $K_1 = 10^{-6}$ dyn, $\alpha = 30$ dyn/cm, $\rho = 1.0$ g/cm^3, $\eta_3 = 1.0$ poise, and $q_\perp$ is chosen such that $\delta^{-1} = (q_\perp l_d)^{-2} = 20\,000$, 2000, 1, and 0.1, respectively. log(δ) in the figure is the natural logarithm.

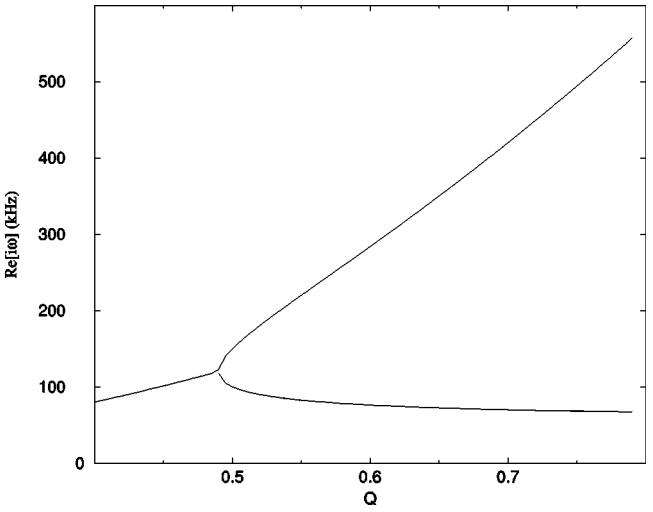

FIG. 4. Decay rates for normal modes with $n=0$ in the $q_\perp l_d \ll 1$ regime. The dimensionless wave vector is defined as $Q = q_\perp d$. The material parameters are chosen as $\eta_3 = 1.0$ *P*, $\rho = 1.0$ g/cm^3, $d = 10$ μm, and $\alpha = 30$ dyn/cm. When the decay rates merge, the system undergoes underdamped motion.

the figure change over many orders of magnitude. Thus, experimentally probing this entire figure may require different scattering probes.

IV. SMECTIC ORDER-PARAMETER AUTOCORRELATION FUNCTION

As a recent numerical study shows [7], the crossover dynamics in a freely standing smectic-*A* film can also be observed in the smectic order-parameter autocorrelation function. For a thermotropic smectic *A* [1,2],

$$\rho(\mathbf{r})=\rho_0+[\langle\phi_1\rangle e^{iq_0z}+\text{c.c.}], \tag{35}$$

where $\langle\phi_1\rangle=|\langle\phi_1\rangle|e^{-iq_0u}$ is the dominant order parameter for the thermotropic smectic-*A* phase and q_0 is essentially the inverse smectic-layer thickness. The autocorrelation function for the dominant order parameter is

$$\langle\phi_1(\mathbf{r}_1,t)\phi_1(\mathbf{r}_2,0)\rangle=|\langle\phi_1\rangle|^2e^{-g(\mathbf{r}_1,\mathbf{r}_2,t)}, \tag{36}$$

where

$$\begin{aligned} g(\mathbf{r}_1,\mathbf{r}_2,t)&=\frac{q_0^2}{2}\langle[u(\mathbf{r}_1,t)-u(\mathbf{r}_2,0)]^2\rangle \\ &=\frac{q_0^2}{2}[\langle u^2(\mathbf{r}_1,t)\rangle+\langle u^2(\mathbf{r}_2,t)\rangle \\ &\quad -2\langle u(\mathbf{r}_1,t)u(\mathbf{r}_2,0)\rangle]. \end{aligned} \tag{37}$$

We shall refer to the first and second terms on the right-hand side of the above equation as the *local part* of g and the third term as the *nonlocal part*. Although the translational invariance in the z direction is broken and the local part depends on z_1 and z_2, only the contribution from the nonlocal part shows true correlation between the layer fluctuations at two different space-time points. The local part will provide the ''counterterms'' for some of the calculations to follow.

It is convenient to express $\langle u(\mathbf{r_1},t)u(\mathbf{r}_2,0)\rangle$ in terms of the normal modes,

$$\begin{aligned} \langle u(\mathbf{r}_1,t)u(\mathbf{r}_2,0)\rangle=\sum_n\int\frac{d^2q_\perp}{(2\pi)^2}c(q_\perp,n,t)e^{i\mathbf{q}_\perp\cdot\mathbf{r}_\perp} \\ \times\psi(q_\perp,n;z_1)\psi(q_\perp,n;z_2), \\ \mathbf{r}_\perp=\mathbf{r}_{1\perp}-\mathbf{r}_{2\perp}. \end{aligned} \tag{38}$$

Each term in the local part of g has the same form as the above but with $\mathbf{r}_\perp=0$, $t=0$, and $\psi(q_\perp,n;z_1)\psi(q_\perp,n;z_2)$ replaced by $\psi^2(q_\perp,n;z_{1(2)})$. As will be shown below, the normal modes which dominate the *nonlocal* part of g also control the asymptotic behavior of g, as summarized in Table II. In the remainder of this section, we discuss entries in this table and compare with existing numerical work [7].

(i) When $r_\perp\ll l_d$, $t\ll\tau_0$, the nonlocal part of g is dominated by $q_\perp l_d\gg1$ modes. The $q_\perp l_d\ll1$ part in g in this short-time limit can be approximated by its value at $t=0$, $r_\perp=0$, and the layer fluctuations are dominated by the $n=0$ modes, which are independent of z_1 and z_2. Hence, there is cancellation with their contribution to the local part. Since the dominant fluctuation for $q_\perp l_d\gg1$ modes comes from those with $n\gg1$, the boundary condition is not important as long as both $\mathbf{r_1}$ and $\mathbf{r_2}$ are sufficiently away from the free surfaces [21]. Therefore, $g(\mathbf{r_1},\mathbf{r_2},t)$ in this limit can be approximated by

TABLE II. Asymptotics of the autocorrelation function.

Condition	Dominant fluctuations	Asymptotic behavior of g
$r_\perp\ll l_d$, $t\ll\tau_0$, and $z_{1(2)}\pm d/2\gg r_\perp^2/\lambda$	$q_\perp l_d\gg1$, $n\gg1$	Eq. (40)
$l_d\ll r_\perp\ll l_c$ and $t\lesssim\tau_0$	$l_c^{-1}\ll q_\perp\ll l_d^{-1}$, $n=0$	Eq. (41)[a]
$t\gg\tau_0$ and $r_\perp\ll l_c$	$q_\perp l_c\ll1$, $n=0$	Eq. (45)[a]
$t/\tau_0\gg(r_\perp/l_c)^2$	$q_\perp l_c\ll1$, $n=0$	Eq. (45)[a]
$l_c\ll r_\perp$ and $t\ll\tau_0$	$q_\perp l_c\ll1$, $n=0$	Eq. (46)[a]

[a] z_1,z_2 dependence ignored.

$$\begin{aligned} g(\mathbf{r}_1,\mathbf{r}_2,t)\approx\frac{1}{d}\sum_{n=0}\int_{l_d^{-1}}\frac{dq_\perp^2}{(2\pi)^2} \\ \times[c(q_\perp,n,0)-c(q_\perp,n,t)\ e^{i\mathbf{q}_\perp\cdot\mathbf{r}_\perp+i(n+1)\pi z/d}], \end{aligned} \tag{39}$$

where $z=|z_1-z_2|$, and we have used periodic boundary conditions in the z direction to simplify the expression. The asymptotic behavior of the above expression is the same as that for a bulk system [6], namely,

$$g(\mathbf{r}_1,\mathbf{r}_2,t)\sim\begin{cases} 2\eta\ln r_\perp, & r_\perp^2/\lambda d\gg z/d \text{ and } r_\perp^2/\lambda d\gg t/\tau_0 \\ \eta\ln z, & z/d\gg r_\perp^2/\lambda d \text{ and } z/d\gg t/\tau_0 \\ \eta\ln t, & z/d\gg r_\perp^2/\lambda d \text{ and } t/\tau_0\gg z/d, \end{cases} \tag{40}$$

where $\eta=k_BTq_0^2/8\pi\sqrt{BK_1}$.

(ii) When $l_d\ll r_\perp\ll l_c$ and $t\lesssim\tau_0$, the relevant modes for the nonlocal part of g have $n=0$ and $l_c^{-1}\ll q_\perp\ll l_d^{-1}$, and they are independent of z_1 and z_2. The z_1 and z_2 dependence comes from the local part of g only; hence, we will ignore it. Similarly to (i), there is cancellation of the contributions of $q_\perp l_c\ll1$ modes between the nonlocal and local parts of g. From Eq. (31), the $r_\perp$- and t-dependent part of g can be expressed as [22]

$$\begin{aligned} \frac{q_0^2}{2}\int_{l_c^{-1}}^{l_d^{-1}}\frac{d^2q}{(2\pi)^2}\frac{k_BT}{2\alpha q_\perp^2}(1-e^{-t/\tau_0}e^{i\mathbf{q}_\perp\cdot\mathbf{r}_\perp}) \\ \approx\frac{k_BTq_0^2}{4\pi\alpha}e^{-t/\tau_0}\left(\ln\frac{r_\perp}{l_c}+\tilde{\gamma}\right)+A_0, \end{aligned} \tag{41}$$

where A_0 is constant. This result indicates that the order-parameter correlation function behaves as $r_\perp^{-\gamma(t)}$ with a time-dependent exponent $\gamma(t)=\exp(-t/\tau_0)k_BTq_0^2/4\pi\alpha$. This particular time-dependent power-law decay has been found theoretically [6] within a discrete model and also numerically [7].

(iii) When $t\gg\tau_0$, $r_\perp\ll l_c$, modes with $q_\perp l_c\gg1$ in the nonlocal part of g all decay away. Similarly to (ii), from Eq. (32) one finds the $r_\perp$- and t-dependent part of g,

$$\frac{q_0^2}{2}\int_0^{l_c^{-1}}\frac{d^2q}{(2\pi)^2}\frac{k_BT}{2\alpha q_\perp^2}[1-\cos(2q_\perp l_c t/\tau_0)\times\exp(-2q_\perp^2 l_c^2 t/\tau_0)\exp(i\mathbf{q}_\perp\cdot\mathbf{r}_\perp)]$$
$$=\frac{k_BTq_0^2}{4\pi\alpha}[I_0(2t/\tau_0)+I_1(2t/\tau_0,r_\perp/l_c)], \quad (42)$$

where

$$I_0(t)=\int_0^1 dQ\,\frac{1-\cos Qt\ \ e^{-Q^2t}}{Q}, \quad (43)$$

$$I_1(t,R)=\int_0^1 dQ\cos Qt\ \ e^{-Q^2t}\frac{1-J_0(QR)}{Q}. \quad (44)$$

Using the appropriate asymptotic behavior of $I_0(t)$ and $I_1(t,R)$ provided in Eqs. (C3) and (C7), one finds that to order $(r_\perp/l_c)^2$, the $r_\perp$- and t-dependent part of g is given by

$$\frac{k_BTq_0^2}{4\pi\alpha}\left\{\ln\frac{t}{\tau_0}+\frac{r_\perp^2}{8l_c^2}\frac{\tau_0}{2t}\times\left[1-\sqrt{\frac{\pi t}{2\tau_0}}e^{-t/2\tau_0}\,\mathrm{erf}\,i\left(\sqrt{\frac{t}{2\tau_0}}\right)+O(e^{-t/2\tau_0})\right]\right\}, \quad (45)$$

where $\mathrm{erf}\,i(x)$ is defined in Eq. (C8). The logarithmic t dependence in the case of $r_\perp=0$ has been seen numerically [7], while the more complicated time dependence of the leading $r_\perp$ term has not been reported.

(iv) When $l_c\ll r_\perp$, the dominant modes in the nonlocal part of g are $n=0$ modes with $q_\perp l_c\ll 1$. The $r_\perp$- and t-dependent part of g is also provided by Eq. (42). The $z_{1\ (2)}$ dependence is ignored as in (iii). Two asymptotic forms follow.

(a) $t/\tau_0\gg(r_\perp/l_c)^2\gg 1$. Using Eqs. (C3) and (C7), one finds that the $r_\perp$ and t dependence of g is the same as case (iii).

(b) $t\ll\tau_0$. From Eqs. (C1) and (C5), one finds that the $r_\perp$- and t-dependent part of g is given by

$$\frac{k_BTq_0^2}{4\pi\alpha}\left[\ln\frac{r_\perp}{l_c}+t\sqrt{\frac{2l_c^3}{\pi r_\perp^3}}\cos\left(\frac{r_\perp}{l_c}-\frac{3\pi}{4}\right)\right]+O(t^2). \quad (46)$$

The $t=0$ behavior in this case has been verified by the numerical work in [7]. However, notice that the time-dependent part oscillates in $r_\perp$ with a characteristic length l_c, which does not appear in the postulated scaling form of Ref. [7], in which the $r_\perp\gg l_c$ regime is not included in the numerical calculation of the order-parameter correlation function [23]. We suggest that further study of the autocorrelation function of the smectic order parameter will reveal this important length.

We have shown the asymptotic behavior of the smectic order-parameter correlation function in various regimes. In cases (i) and (ii), the behavior agrees with existing numerical approaches. Although the $r_\perp=0$ case in (iii) and (iv),(a) as well as the $t=0$ case in (iv),(b) are discussed in Ref. [7], additional numerical and/or experimental studies are required to find the interesting $r_\perp$ and t dependence of the autocorrelation function and especially the length, l_c, which characterizes the long-wavelength underdamped dynamics.

V. CONCLUDING REMARKS

The layer dynamics of a freely standing smectic-A film have been determined by analyzing the response functions for the surface displacement. By determining the positions of the poles of the response functions in the complex ω plane, we find not only the frequencies but also the spatial configurations for the hydrodynamic modes of the system. The fact that u and v_z are two nonseparable hydrodynamic variables, in general, is reflected in the form of the dynamic correlation function for u.

When $q_\perp l_d\ll 1$, the internal structure of the layers is not important for the system. For fixed $q_\perp$, one pair of normal modes dominates the statics and dynamics of the system. Furthermore, the layer fluctuations and the characteristic frequencies for these important normal modes have essentially no dependence on the elasticity of the smectic layers, i.e., only surface tension and viscosity are important. To extract information on the internal structure of the system, i.e., the smectic layers, it is necessary to excite other normal modes. As discussed in Ref. [11], exciting the $n=1$ modes provides information on the crossover behavior of the system from a quasi-two-dimensional system to a three-dimensional system. This can be done by adjusting the experimental parameters such that $q_\perp l_d$ is of order unity. The mode structure for the system in the regime $q_\perp l_d\gg 1$ is similar to that of bulk systems. However, the characteristic time scales for the hydrodynamic modes will now acquire surface and finite thickness corrections as well.

The dynamic crossover behavior can also be found in the smectic order parameter autocorrelation function. In general, for $q_\perp l_d\gg 1$, $t/\tau_0\ll 1$ this autocorrelation function is similar to a bulk smectic-A system. For long wavelength or large time, the behavior is controlled by l_d, l_c, and τ_0, and is similar to an ordinary fluid film. We suggest that further experimental or numerical studies will reveal some interesting time or $r_\perp$ dependence of the autocorrelation function.

To summarize, we have explored the dynamic properties of a freely standing smectic-A film in the linear regime. It is shown that existing experiments were performed in the limit where only the two-dimensional character of the film can be detected. Future experiments on the dynamical correlations of the smectic layers may reveal the crossover behavior of the system to a regime in which layer elasticity begins to play a role. The behavior of the autocorrelation function for the smectic order parameter is also discussed and compared with an existing numerical study. Our analysis provides the basis for the numerical results and provides a clear conceptual picture showing the need for additional studies to explore interesting behavior. Finally, our work also provides the formulation for a future theoretical study of the dynamics of a freely standing smectic-A film far from equilibrium, where experiments show behavior which is drastically different from that of a bulk system [9]. The effect of finite thickness and surface tension will have to play a central role in a theory which describes such dynamical behavior.

ACKNOWLEDGMENTS

We thank Professor X-l. Wu for helpful discussions. H.-Y.C. is grateful for support from the University of Pittsburgh. D.J. is grateful for the support of the NSF under Contract No. DMR9217935.

APPENDIX A

We discuss permeation processes in free-standing smectic-*A* films in this appendix. We look for a solution of the equations of motion with boundary conditions and external forces given in Sec. II. In the long-wavelength, low-frequency limit [13] the solution is of the form

$$u = u_{\rm el} + u_p , \tag{A1}$$

where

$$u_{\rm el}(\mathbf{r},t) = u_S(\mathbf{q}_\perp,\omega)\cos[q_z(q_\perp,\omega)z]e^{i\mathbf{q}_\perp\cdot\mathbf{r}_\perp - i\omega t} + u_A(\mathbf{q}_\perp,\omega)\sin[q_z(q_\perp,\omega)z]e^{i\mathbf{q}_\perp\cdot\mathbf{r}_\perp - i\omega t} \tag{A2}$$

is the approximate solution used in the text. It is independent of the permeation constant. The second contribution

$$u_p(\mathbf{r},t) = [u_p^+(\mathbf{q}_\perp)e^{+(1+i)p(q_\perp)(z-d/2)} + \text{c.c.}]e^{i\mathbf{q}_\perp\cdot\mathbf{r}_\perp - i\omega t} + [u_p^-(\mathbf{q}_\perp)e^{-(1+i)p(q_\perp)(z+d/2)} + \text{c.c.}]e^{i\mathbf{q}_\perp\cdot\mathbf{r}_\perp - i\omega t} \tag{A3}$$

contains an inverse length, $p(q_\perp) = \sqrt{q_\perp/2(\zeta_P\eta_3)^{1/2}}$, which characterizes the decay of permeation away from the free surfaces. In typical materials $p(q_\perp) \gg q_\perp \gg q_z$ in the low-frequency, long-wavelength regime [13]. The amplitudes $u_p^\pm$ contain the contributions from permeation and are related to $u_{\rm el}$ through the full boundary conditions.

From Eqs. (9) and (7) we find that $|u_p^\pm| \ll |u_{\rm el}|$, i.e., the contribution of permeation to the layer displacement is small [11]. Then Eq. (6) leads to

$$\zeta^\pm \approx [u_{\rm el}]_{z=\pm d/2} . \tag{A4}$$

It is straightforward to show that the elastic free energy is

$$\begin{aligned} F &= \frac{1}{2}\int dV\left\{B\left(\frac{\partial u}{\partial z}\right)^2 + K_1\left(\frac{\partial^2 u}{\partial x^2} + \frac{\partial^2 u}{\partial y^2}\right)^2\right\} \\ &\quad + \sum_{i=+,-}\frac{1}{2}\int dS^i\,\alpha\left\{\left(\frac{\partial \zeta^i}{\partial x}\right)^2 + \left(\frac{\partial \zeta^i}{\partial y}\right)^2\right\} \\ &\approx \frac{1}{2}\int dV\left\{B\left(\frac{\partial u_p}{\partial z}\right)^2 + B\left(\frac{\partial u_{\rm el}}{\partial z}\right)^2 + K_1\left(\frac{\partial^2 u_{\rm el}}{\partial x^2} + \frac{\partial^2 u_{\rm el}}{\partial y^2}\right)^2\right\} \\ &\quad + \sum_{i=+,-}\frac{1}{2}\int dS^i\,\alpha\left\{\left(\frac{\partial u_{\rm el}}{\partial x}\right)^2 + \left(\frac{\partial u_{\rm el}}{\partial y}\right)^2\right\}_{z=\pm d/2} . \end{aligned} \tag{A5}$$

In the linear theory the contribution from permeation can be separated from the contribution from $u_{\rm el}$. Since $|u_p^\pm| \ll |u_{\rm el}|$ in the regime where we perform this long-wavelength analysis, we can neglect the u_p part. However, it is $u_{\rm el}$, not the full displacement u, that can be expanded as a linear combination of the normal modes discussed in the text and satisfies BC2′ [Eq. (19)]. When u_p is included, the permeation force $B\partial u/\partial z$ vanishes on the free surfaces due to the existence of u_p. This has been noted in the literature [18,19] but has not been discussed in previous studies of statics and dynamics of free standing smectic-A films [3,6,7].

APPENDIX B

In this appendix we calculate the dynamic correlation functions for u and v_z. We consider the $u_{\rm el}$ part only; the u_p part simply corresponds to the permeation mode discussed in the literature [1,10]. Our starting point is the equations of motion, i.e., Eqs. (3) and (4), and the dynamics of the normal modes labeled by $(\mathbf{q}_\perp, n)$ are considered. Eliminating the pressure via the incompressibility condition, we find that there are two diffusive modes associated with v_x and v_y, but v_x and v_y decouple from v_z and u [2]. Neglecting permeation [20], the equations for v_z and u can be expressed as

$$\frac{\partial}{\partial t}\begin{pmatrix} u \\ v_z \end{pmatrix} = \begin{pmatrix} 0 & 1 \\ -R & -D \end{pmatrix}\begin{pmatrix} u \\ v_z \end{pmatrix}, \tag{B1}$$

where

$$D = \frac{1}{\rho}\ \eta_3 q_\perp^2 \tag{B2}$$

represents the dissipative part and

$$R = \frac{1}{\rho}\ (Bq_z^{(n)2} + K_1 q_\perp^4) \tag{B3}$$

represents the reactive part. We have used the fact that $q_z^{(n)} \ll q_\perp$ for all n in the regime of our calculation to simplify the expressions. The eigenvectors of the above matrix equation are

$$\Phi_\pm = \frac{1}{\sqrt{1 + [i\omega_\pm(q_\perp, q_z^{(n)})]^2}}\begin{pmatrix} 1 \\ -i\omega_\pm(q_\perp, q_z^{(n)}) \end{pmatrix}, \tag{B4}$$

with eigenvalues $-i\omega_\pm(q_\perp, q_z^{(n)})$ given in Eq. (12). Straightforward algebra leads to the following relation:

$$\begin{pmatrix} u(t) \\ v_z(t) \end{pmatrix} = \frac{1}{i\omega_+ - i\omega_-}\begin{pmatrix} [i\omega_+ e^{-i\omega_- t} - i\omega_- e^{-i\omega_+ t}]u(0) + [e^{-i\omega_- t} - e^{-i\omega_+ t}]v_z(0) \\ -\omega_+\omega_-[e^{-i\omega_+ t} - e^{-i\omega_- t}]u(0) + [i\omega_+ e^{-i\omega_+ t} - i\omega_- e^{-i\omega_- t}]v_z(0) \end{pmatrix}, \tag{B5}$$

where we used simplified notation, $\omega_{\pm}=\omega_{\pm}(q_{\perp},q_z^{(n)})$, $u(t)=u(q_{\perp},n,t)$, $v_z(t)=v_z(q_{\perp},n,t)$, etc. From this one concludes that the dynamic correlation function for u is

$$\begin{aligned}\langle u(q_{\perp},n,t)\ \ u(-q_{\perp},m,0)\rangle &= \delta_{nm}\ \frac{i\omega_+e^{-i\omega_-t}-i\omega_-e^{-i\omega_+t}}{i\omega_+-i\omega_-}\langle|u(q_{\perp},n,0)|^2\rangle \\ &= \delta_{nm}\ \frac{i\omega_+e^{-i\omega_-t}-i\omega_-e^{-i\omega_+t}}{i\omega_+-i\omega_-}\frac{k_BT}{Bq_z^{(n)2}+K_1q_{\perp}^4},\end{aligned} \tag{B6}$$

as given in Sec. II. The calculation of the correlation function for v_z is similar to that for u.

APPENDIX C

We discuss some asymptotic behavior of the integrals I_0, I_1 in this appendix. $I_0(t)$ is defined in Eq. (43). In the $t\ll 1$ limit, expanding around $t=0$ to lowest order, one finds

$$I_0(t)=\frac{t}{2}+O(t^2). \tag{C1}$$

When $t\gg 1$, one reexpresses Eq. (43) as

$$I_0(t)=\int_0^1 dx\,\frac{1-(\cos x)\exp(-x^2/t)}{x} + \int_1^t\frac{dx}{x}-\int_1^t dx\,\frac{(\cos x)\exp(-x^2/t)}{x}. \tag{C2}$$

The first and the third terms on the right-hand side tend to constants in the large-t limit,

$$\int_0^1 dx\,\frac{1-(\cos x)\exp(-x^2/t)}{x}\approx 0.24,$$

$$-\int_1^t dx\,\frac{(\cos x)\exp(-x^2/t)}{x}\approx 0.34,\quad t\gg 1.$$

Hence

$$I_0(t)\approx 0.58+\ln t,\quad t\gg 1. \tag{C3}$$

Next we examine the asymptotic behavior of $I_1(t,R)$, which is defined in Eq. (44). When $R\ll 1$, $t\ll 1$, expanding $I_1(t,R)$ around $R=0$, $t=0$ yields

$$I_1(t,R)=\frac{R^2}{8}-\frac{R^2t}{12}+O(t^2,R^4). \tag{C4}$$

When $R\gg 1$, $t\ll 1$, expanding $I_1(t,R)$ around $t=0$ leads to

$$\begin{aligned}I_1(t,R)&=\int_0^1 dQ\ \ \frac{1-Q^2t}{Q}[1-J_0(QR)]+O(t^2)\\ &\approx\tilde{\gamma}+\ln R+\left(-\frac{1}{2}+\frac{J_1(R)}{R}\right)t+O(t^2)\\ &\approx\tilde{\gamma}+\ln R+\left[-\frac{1}{2}+\sqrt{\frac{2}{\pi R^3}}\cos\left(R-\frac{3\pi}{4}\right)\right]t,\end{aligned} \tag{C5}$$

where

$$\tilde{\gamma}=\int_0^1\frac{dx}{x}[1-J_0(x)]-\int_1^{\infty}\frac{dx}{x}J_0(x)\approx -0.116, \tag{C6}$$

and J_1 is the Bessel function of the first kind. The identity $d(xJ_1(x))/dx=xJ_0(x)$ and limit $J_1(x)\approx\sqrt{2/\pi x}\cos[x-3\pi/4]$ for $x\gg 1$ have been used. When $t\gg R^2$ and $t\gg 1$, a change of variables yields

$$\begin{aligned}I_1(t,R)&=\int_0^{\sqrt{t}}\frac{dx}{x}\cos(x\sqrt{t})\exp(-x^2)\left[1-J_0\left(\frac{xR}{\sqrt{t}}\right)\right]\\ &\approx\frac{R^2}{4}\left[\frac{1-e^{-t}\cos t}{2t}-\frac{\sqrt{\pi}e^{-t/4}}{4\sqrt{t}}\,\mathrm{erf}\ i\left(\frac{\sqrt{t}}{2}\right)\right],\end{aligned} \tag{C7}$$

where the Bessel function has been expanded and

$$\mathrm{erf}\ i(x)=\mathrm{erf}(ix)/i. \tag{C8}$$

For large x using standard manipulations on the error function of a complex argument, one has

$$\mathrm{erf}\,i(x)\approx\exp(x^2)[(1/\sqrt{\pi}x)+(1/2\sqrt{\pi}x^3)+O(x^{-4})]$$

[24].

[1] P.G. de Gennes and J. Prost, *The Physics of Liquid Crystals* (Clarendon Press, Oxford, 1993).

[2] P.M. Chaikin and T.C. Lubensky, *Principles of Condensed Matter Physics* (Cambridge University Press, Cambridge, 1995).

[3] E.A.L. Mol, J.D. Shindler, A.N. Shalaginov, and W.H. de Jeu, Phys. Rev. E **54**, 536 (1995).

[4] A. Poniewierski and R. Hołyst, Phys. Rev. B **47**, 9840 (1993), and references therein.

[5] J.B. Fournier, J. Phys. II **6**, 985 (1996).

[6] A. Poniewierski, R. Hołyst, A.C. Price, L.B. Sorensen, S.D. Kevan, and J. Toner, Phys. Rev. E **58**, 2027 (1998).

[7] A. Poniewierski, R. Hołyst, A.C. Price, and L. B. Sorensen, Phys. Rev. E **59**, 3048 (1999).

[8] A.C. Price, L.B. Sorensen, S.D. Kevan, J. Toner, A. Poniewierski, and R. Hołyst, Phys. Rev. Lett. **82**, 755 (1999).

[9] D. Dash and X-l. Wu, Phys. Rev. Lett. **79**, 1483 (1997).

[10] P.C. Martin, O. Parodi, and P.S. Pershan, Phys. Rev. A **6**, 2401 (1972).

[11] H-Y. Chen and D. Jasnow, Phys. Rev. E **57**, 5639 (1998).

[12] Orsay Group on Liquid Crystals, J. Phys. (Paris) **36** (Suppl. C1), 305 (1975).

[13] We consider the regime where $\lambda q_{\perp}\ll 1$, $\zeta_p\eta_3q_{\perp}^2\ll 1$ (small boundary layer [1]). Also we assume $|\omega|\eta_3/B\ll 1$ and $|\omega|/q_{\perp}\ll\sqrt{B/\rho}$, the latter inequality stating that the velocity of the surface wave is small compared to the typical velocity of ''second sound.''

[14] To make a connection with a bulk smectic-*A* system, the notation we choose in this paper is different from Ref. [11];

however, the calculation is along the same lines.
[15] Notice that for a typical material the factor $g \sim O(1)$.
[16] K. Miyano, Phys. Rev. A **26**, 1820 (1982); P. Pierański *et al.*, Physica A **194**, 364 (1993); R. Hołyst, Phys. Rev. A **46**, 6748 (1992).
[17] These normal modes correspond to the peak of the surface peristaltic mode discussed in Ref. [11].
[18] M. Kléman, *Points, Lines, and Walls* (John Wiley & Sons, New York, 1983); M. Kléman and O. Parodi, J. Phys. (Paris) **36**, 617 (1975).
[19] A. Rapini, Can. J. Phys. **53**, 968 (1975).
[20] Permeation has a negligible effect on the mode structure of the u_{el} part.
[21] The boundary condition is not important when the distances of $\mathbf{r}_1$ and $\mathbf{r}_2$ to the free surfaces are large compared to the inverse of the typical value of $q_z^{(n)}$, which is on the order of $\lambda q_\perp^2 \sim \lambda / r_\perp^2$.
[22] A similar integral also appears in Ref. [6].
[23] Checking the material parameters used in Ref. [7], one finds that their numerical work covers up to $r_\perp \sim l_c$.
[24] S. Wolfram, *Mathematica*, 3rd ed. (Addison-Wesley, New York, 1996); *Handbook of Mathematical Functions*, edited by M. Abramowitz and I. A. Stegun (Dover, New York, 1972), Chap. 7.